

**Endogenous Adipocyte ApoE is Co-localized with Caveolin at the  
Adipocyte Plasma Membrane**

**Lili Yue\* and Theodore Mazzone†**

**\*Department of Medicine**

**†Departments of Medicine, Pharmacology, and Kinesiology and Nutrition**

**University of Illinois at Chicago**

**Chicago, Illinois 60612**

**Running title:** Adipocyte apoE and caveolae

**Correspondence to:**

Theodore Mazzone, MD,  
Section of Endocrinology, Diabetes and Metabolism (M/C 797)  
University of Illinois at Chicago  
1819 W. Polk Street  
Chicago, IL 60612  
Tel. 312/996-7989  
Fax. 312/413-0437  
Email: tmazzone@uic.edu

**Abbreviations:** EKO, apoE knockout; WT, wild-type; M $\beta$ CD, methyl- $\beta$ -cyclodextrin; DSP, Dithiobis[succinimidyl propionate]; GFP, green fluorescent protein; TG, triglyceride; CH, cholesterol; DIC, differential interference contrast; GM1, N-acetylneuraminyl tetrasylceramide; caveolin-1, cav-1; CBDE, cav-1 binding domain in human apoE; B-CBDE, biotin labeled cav-1 binding domain in human apoE; CBDE-mut, mutant cav-1 binding domain in human apoE

## **Abstract**

Apolipoprotein E is well-established as a secreted protein that plays an important role in systemic lipoprotein metabolism and vascular wall homeostasis. Recently, endogenous expression of apoE in adipocytes has been shown to play an important role in adipocyte lipoprotein metabolism and gene expression consistent with a non-secreted cellular itinerary for apoE. We designed studies to evaluate if adipocyte apoE was retained as a constituent protein in adipocytes, and to identify a cellular retention compartment. Using confocal microscopy, co-immunoprecipitation, and sucrose density cellular fractionation, we establish that endogenous apoE shares a cellular itinerary with the constituent protein caveolin-1. Altering adipocyte caveolar number by modulating cellular cholesterol flux or altering caveolin expression regulates the distribution of cellular apoE between cytoplasmic and plasma membrane compartments. A mechanism for co-localization of apoE with caveolin was established by demonstrating a non-covalent interaction between an aromatic amino acid-enriched apoE N-terminal domain with the caveolin scaffolding domain. Absent apoE expression in adipocytes alters caveolar lipid composition. These observations provide evidence for an interaction between two proteins involved in cellular lipid metabolism in a cell specialized for lipid storage and flux, and rationalize a biological basis for the impact of adipocyte apoE expression on adipocyte lipoprotein metabolism.

**Supplementary Key Words:** adipocytes, caveolin, apolipoprotein E, adipose tissue, caveolae, obesity

## Introduction

Obesity is an important and increasingly prevalent health problem that predisposes to metabolic and cardiovascular disease (1,2). Recently, there has been increased attention focused on adipocytes and adipose tissue, and it has become clear that they constitute a metabolically complex organ with a major role in regulation of organismal metabolism (3,4). Different from many cell types, adipocytes have adapted to store large amounts of lipid and experience substantial lipid flux as part of their differentiated function. This cell type expresses two proteins, caveolin-1 (cav-1) and apoE, at high level that are likely important for this specialization. Cav-1 is a sterol-binding integral membrane protein that is highly expressed in adipocytes and that specifies the organization of the adipocyte plasma membrane into ultra-structurally distinct lipid-rich domains termed caveolae (5-8). It is been estimated that up to 30% of adipocyte plasma membrane is found in caveolae. These structures serve an endocytic function, and may be important for insulin signal transduction and Glut-4 translocation (5-12). A subset of caveolae in adipocytes has been shown to synthesize triglyceride (TG) and to form lipid droplets, and caveolae are an important site of fatty acid internalization by adipocytes (6,13). Cav-1 knockout mice have decreased adipose tissue mass, small lipid-poor adipocytes, and are resistant to diet-induced obesity (10). At the same time, they have increased circulating lipids. These *in vivo* observations are consistent with an inability to accumulate adipose tissue lipid in cav-1 knockout mice.

ApoE is a phospholipid binding protein that is well-characterized as a secreted protein from hepatocytes and macrophages, and that has an important role in systemic lipoprotein metabolism and vessel wall homeostasis. Its high-level expression by adipocytes was demonstrated two decades ago (14). More recently, additional information regarding these

issues has become available. Nutritional status, peptide hormones, LXR agonists, and PPAR $\gamma$  agonists regulate adipocyte apoE expression *in vitro* and *in vivo* (15-20). Further, an important role for endogenous adipocyte apoE in adipocyte lipid metabolism and gene expression has been demonstrated (21-23). Adipocytes freshly isolated from apoE knockout (EKO) mice are small and lipid-poor, and this phenotype is maintained after a 2-week incubation in culture in the presence of apoE-containing lipoproteins. Moreover, this phenotype can be reversed in cultured adipocytes by adenoviral-mediated expression of apoE (21). Even more importantly, after transplantation of EKO adipose tissue into wild-type (WT) recipients, EKO adipocytes remain smaller and lipid-poor compared to adipocytes isolated from similarly transplanted WT adipose tissue (22). Therefore, lack of endogenous apoE expression limits the ability of adipocytes to acquire lipid from circulating lipoproteins even in a WT *in vivo* environment and with WT levels of circulating apoE. Multiple changes in adipocyte gene and protein expression in EKO adipocytes have also been documented (21). One of the genes most affected in EKO adipocytes is cav-1. Cav-1 mRNA levels are significantly reduced in EKO adipocytes, and cav-1 protein expression is suppressed by 50% (21-23). We have also documented a significant defect in fatty acid internalization by EKO adipocytes (23). Provocatively, this defect can be corrected by increasing cav-1 expression using viral transduction in EKO adipocytes.

The above observations suggest a non-secreted role for apoE as a constituent cellular protein in adipocytes, and further suggest an important functional interaction between apoE and caveolin. In these studies we evaluate these hypotheses and provide evidence that adipocyte apoE and caveolin share a common cellular destination at the adipocyte plasma membrane.

## **Experimental Procedures**

### Materials

3T3-L1 cells were obtained from American Type Culture Collection (Manassas, VA). Linoleic acid and HPTLC standards were purchased from Nu-Chek Prep (Elysian, MN). EGTA, poly-L-lysine and methyl- $\beta$ -cyclodextrin (M $\beta$ CD) were purchased from Sigma. Mouse monoclonal anti-human apoE antibodies were purchased from Abcam (Cambridge, MA). Rabbit anti-cav-1 antibody and ExactaCruz<sup>TM</sup> C were from Santa Cruz Biotechnology (Santa Cruz, CA). Alexa Fluor 594 donkey anti-rabbit, Alexa Fluor 488 donkey anti-mouse conjugated secondary antibodies, Image-iT FX signal enhancer and ProLong Gold antifade reagent were purchased from Invitrogen (Carlsbad, CA). Liberase Blendzyme 3 was purchased from Roche Applied Science (Indianapolis, IN). Dithiobis[succinimidyl propionate] (DSP) was from Thermo Scientific (Rockford, IL). Other materials were from previously described sources (15,18-20,23).

### Cell Isolation and Culture

All animal protocols were approved by the Institutional Animal Care and Use Committee of the University of Illinois at Chicago. Male Sprague-Dawley rats weighing 250-275g were from Charles River Laboratory. After euthanasia, intra-abdominal fat pads were removed and washed in sterile PBS. The fat pads were cut into 1-2mm pieces and digested using 0.5mg/ml Liberase Blendzyme 3 in DMEM in 10% FBS for 1h at 37°C in a shaking water bath. Preadipocytes were isolated and differentiated in culture as previously described in detail (21). 3T3-L1 cells were maintained and differentiated in culture as previously described and were used for experiments between days 8-13 after completion of a 3-day incubation in differentiation

medium. For recovery of mature adipocytes from freshly isolated adipose tissue, intra-abdominal fat pads were recovered from WT or EKO mice and digested as described above for rat fat pads. Mature adipocytes were isolated in a floating fraction after filtering and centrifugation of the digestate as previously described (21).

For experimental incubations, fully differentiated 3T3-L1 adipocytes or primary adipocytes were washed once in serum-free medium and incubated in DMEM with 100 $\mu$ M BSA for 2h. The cells were then changed to this medium alone or with 10 $\mu$ g/ml of cholesterol (CH) (dissolved in ethanol), 10mM M $\beta$ CD, or 250 $\mu$ M of albumin-bound fatty acid (FFA:BSA molar ratio 2.5:1) for the times indicated in the figure legends.

#### Immunofluorescence Staining

Primary or 3T3-L1 adipocytes were cultured and differentiated as described above on chamber slides (Electron Microscopy Sciences, Hatfield, PA), or glass coverslips. The slides were rinsed 3 times with PBS, and fixed for 15 min in freshly prepared 4% formaldehyde. Cells were then permeabilized with 0.1% Triton X-100 in PBS for 5 min at room temperature. The cells were initially blocked with Image-iT FX reagent for 30 min and then further blocked with 3% BSA in PBS for 1h at room temperature. The cells were then incubated with anti-cav-1 antibody (1:500 dilution) and/or anti-apoE monoclonal antibody (1-100 dilution) in blocking buffer for 1h at room temperature. After multiple washes, the cells were incubated with Alexa Fluor 594 conjugated donkey anti-rat (1:400) and/or Alexa Fluor 488 conjugated donkey anti-mouse (1:400) for 1h. The slides were mounted with ProLong Gold antifade reagent, and nuclei were stained with DAPI to be examined by confocal microscopy.

For some studies, endogenously synthesized apoE was detected using an apoE-green fluorescent protein (GFP) fusion protein. The apoE-GFP fusion construct was assembled using the pAcGFP1-N Infusion Ready Vector (Clontech, Mountain View, CA) according to the manufacturer's instructions. The sequence of the construct was verified by the UIC DNA Sequencing Core facility. 3T3-L1 adipocytes grown on chamber slides were transiently transfected to express the apoE-GFP plasmid using Lipofectamine 2000 according to the manufacturer's instructions. After 48h, the cells were fixed and used for confocal microscopy, or fixed and stained with anti-cav-1 for use in confocal microscopy.

#### Isolation of Purified Plasma Membrane Sheets

3T3-L1 adipocytes grown on coverslips were serum-starved for 2h, and then treated with 10 $\mu$ g/ml CH or 10 $\mu$ M M $\beta$ CD for 50 min. Plasma membrane sheets were prepared as described with some modifications (24). Briefly, cells were washed twice with PBS, incubated in 0.5mg/ml poly-L-lysine/PBS for 30 sec, and then incubated for 20 sec in hypotonic solution (solution A diluted 1:3 see below). The coverslips were then placed in solution A (7mM KCL, 5mM magnesium chloride, 3mM EGTA, 30mM HEPES, pH 7.5), and sonicated for 2 sec with a Vibracell 3mm microtip probe (power setting at 35%). The sheets on the coverslips were fixed for 30 min in hypotonic buffer supplemented with 4% formaldehyde, washed in PBS, blocked and stained as described above.

#### Western Blot

Cellular proteins for Western blot were solubilized in 1% Triton X-100 as previously described in detail (15). Protein concentration was measured by Bio-Rad DC Protein Assay.

Equal amounts of protein were separated on 10-14% SDS-PAGE gels and transferred to nitrocellulose membranes. After blocking and incubation with primary antibodies, nitrocellulose membranes were incubated with horseradish peroxidase-coupled donkey anti-rabbit IgG, or donkey anti-goat IgG. The bands were detected and quantitated using chemiluminescence as described previously (15).  $\beta$ -actin was used as loading control for Western blots of total cell lysates.

#### *Cav-1 Knockdown*

SureSilencing<sup>TM</sup> mouse cav-1 shRNA and control plasmids were purchased from SA Biosciences (Frederick, MD). The cav-1 shRNA4 (ACCAGAAGGGACACACAGTTT) was used for all knockdown experiments. 3T3-L1 adipocytes were transiently transfected with this construct using Lipofectamine following the manufacturer's protocols.

#### *Sodium Carbonate Extraction and Sucrose Gradient Isolation of Caveolae*

The procedure to isolate adipocyte caveolae was based on the detergent-free protocol developed by Song et al (25). Briefly, after the treatments indicated in the figure legends, adipocytes were washed with ice cold PBS, scraped into 2ml of 500mM sodium bicarbonate (pH 11) with protease inhibitor cocktail. Cells were homogenized with 20 strokes in a dounce homogenizer and then sonicated with three 20 sec bursts at 35% energy. Equal amounts of protein in each homogenate was adjusted to 45% sucrose by adding 90% sucrose in Tris buffer. Four ml of this solution was placed at the bottom of an ultracentrifuge tube, and overlaid with 4ml of 35% sucrose and 4ml of 5% sucrose in buffer containing 250mM sodium bicarbonate, 150mM sodium chloride, and 25mM Tris. The gradient was spun at 39,000rpm for 18h in an

SW41 rotor (Beckman Instruments, Palo Alto, CA). A light-scattering band confined to the 5-35% sucrose interface was observed that contained plasma membrane caveolae, but excluded higher-density plasma membranes. Twelve fractions (1ml each) were collected from the top (lower density) of the tube. The light-scattering band was generally found in fractions 3-5. Two hundred  $\mu$ l of each fraction was precipitated with 12.5% trichloroacetic acid and dissolved in 2x Laemmli SDS sample buffer to be used for Western blot as described above.

### Co-Immunoprecipitation

For non-denaturing immunoprecipitation, cell lysates were prepared in 50mM Tris (pH 7.4), 150mM NaCl, 0.25% sodium deoxycholate, 2mM EDTA, and 1% Triton X-100. For denaturing immunoprecipitations after cross-linking, cell lysates were prepared in 30mM Tris (pH 7.4), 150mM NaCl, 1% sodium deoxycholate, 2% SDS, and 1% Triton X-100.

Denaturing immunoprecipitations after cross-linking were performed as previously described in detail using a polyclonal antiserum to apoE or cav-1, except that reducing agent was omitted from the cell lysis buffer (26). Cross-linking was achieved using the cell permeant thiol cleavable homobifunctional cross-linker, DSP (1.2nM spacing arm), according to the manufacturer's instructions. After immunoprecipitation, 5% beta mercaptoethanol was included in the sample buffer to cleave the link between apoE and cross-linked proteins prior to separation on an SDS gel.

Non-denaturing immunoprecipitations were conducted in low-detergent lysis buffers (above), using the ExactaCruz<sup>TM</sup> C: SC 45040 kit (Santa Cruz Biotechnologies, Inc., Santa Cruz, CA) according the manufacturer's instructions. The primary antibody was goat polyclonal anti-apoE or rabbit polyclonal anti-cav1. Species-appropriate non-immune serum was used in control

immunoprecipitates to validate specificity of results. After separation on SDS-PAGE, immunoprecipitated proteins were analyzed by Western blot for apoE and cav-1.

#### Lipid Extraction and High Performance TLC

Mature floating adipocytes were recovered from WT or EKO adipose tissue as described above. Caveolar fractions were isolated on discontinuous sucrose gradients and 100 $\mu$ g of caveolar protein was used for lipid extraction in chloroform/methanol (2:1; v/v). The lipid extracts were dried and spotted on HPLTC plates (silica gel 60 F<sub>254</sub>, Merck, Rahway, NJ) The plates were first developed in a solvent system of chloroform/methanol/acetic acid/water (50:37.5:3.5:2). This developing solution was replaced when the solvent front reached half way up the plate to hexane/diethyl ether/acetic acid (80:20:1.5). The lipids were visualized using 10% phosphomolybdic acid in ethanol and heating for 5 min at 110°C. Lipids were identified using lipid standards, and lipid distribution in each lane was quantified by densitometric analysis. The density values for a specific lipid species were averaged across 3 different experiments, and the mean density value for a specific lipid in the control fractions was assigned a value of 100. Density values from individual gels were then expressed relative to this to give rise to relative values for mean  $\pm$  SD shown in Fig. 6.

#### ApoE-Cav-1 Binding Assay

Binding of apoE to cav-1 was determined using a previously described approach (27). A putative aromatic amino acid enriched cav-1 binding domain in human apoE (CBDE, amino acids 41-60: GQRWELALGR FWDYLRWVQT), and a biotin labeled CBDE (B-CBDE), and a mutant CBDE (CBDE-mut) in which all aromatic amino acids were changed to glycine, were

synthesized by Biomatik Corp. (Ontario, Canada). 3T3-L1 adipocyte extracts were incubated in non-denaturing immunoprecipitation lysis buffer with protease inhibitor cocktail for 30 min. Cell extracts (20  $\mu$ g protein) were incubated with B-CBDE (at the concentrations noted in the figure legends) for 90 min at 4°C. For competition assays, cell extracts were preincubated with the indicated concentration of competitor (native or mutated CBDE) for 90 min, and then 1  $\mu$ M of B-CBDE for an additional 90 min. After these incubations, the biotin-labeled apoE complex was immobilized on NeutrAvidin beads (Pierce) during an incubation at room temperature for 60 min with end-over-end mixing. After the beads were extensively washed, the biotin-labeled apoE complex was released from the beads in an elution buffer containing 2XSDS-PAGE sample buffer with 50 mM DTT. This eluate was then used for Western blot and the amount of cav-1 bound to apoE was detected using an antibody to cav-1.

## Results

Figure 1 shows a series of confocal images examining the cellular distribution of apoE and cav-1 employing different experimental models. Figure 1A uses primary cultures of differentiated rat adipocytes incubated for 2h in basal medium, or this medium plus 10 $\mu$ g/ml CH before staining with apoE or cav-1 antibodies for confocal microscopy. Light images of the cells or cell clusters used for the immunofluorescence studies are given in the right-hand column. In basal medium, apoE can be found at the cell surface but is predominantly localized around three large lipid droplets in the cytoplasmic space. Cav-1 is primarily localized on the plasma membrane. There is a small amount of overlap in the plasma membrane between apoE and cav-1 in the merged image. A 2h pre-incubation in CH, however, leads to a dramatic shift in apoE cellular distribution from an intracellular to plasma membrane location. After the CH incubation, the majority of apoE is localized in the plasma membrane and can be co-localized with cav-1.

Figure 1B shows a similar series of images and incubations, but now using the 3T3-L1 mouse adipocyte cell model, and including an incubation in 10mM M $\beta$ CD. Again, light images of single cells used for staining are in the right-hand column. As in the rat primary adipocyte model, CH leads to a significant redistribution of most of the intracellular apoE to the plasma membrane, and to its co-localization with cav-1 in the plasma membrane. Incubation in M $\beta$ CD to remove CH leads to movement of most apoE to the interior of the cell, and loss of co-localization with cav-1.

Figure 1C shows results using the 3T3-L1 cell model, but in this case endogenous cellular apoE is tracked after expression of an apoE-GFP fusion protein in order to specifically localize endogenously synthesized apoE. The dramatic redistribution of apoE to the plasma

membrane and its co-localization with cav-1 after incubation with CH again is clearly demonstrated.

For the images presented in Fig. 1D, plasma membrane sheets were prepared from 3T3-L1 cells (as described in Methods) after incubation of intact cells in basal medium or basal medium plus CH, or plus M $\beta$ CD. Incubation of intact 3T3-L1 cells with CH increases the amount of apoE and cav-1 detected in plasma membrane sheets and leads to substantial co-localization of apoE and cav-1. On the other hand, incubation with M $\beta$ CD to remove plasma membrane CH reduces co-localization of apoE and cav-1 in plasma membrane sheets.

Immunofluorescent staining and confocal microscopy (Fig. 1) demonstrate that apoE and cav-1 can be co-localized to the plasma membrane, and that the degree of co-localization is sensitive to cellular CH flux. Fig. 2 examines co-localization of cav-1 and apoE using a co-immunoprecipitation experimental approach. In Fig. 2A, cells were incubated in basal medium (100 $\mu$ M BSA) for 2h prior to lysis. Lysates were used for immunoprecipitations containing non-immune serum or polyclonal antisera to cav-1 as indicated. Where indicated, the reducible cell permeant cross-linker DSP was incubated with cells prior to lysis. The immunisolated proteins were then utilized for Western blot of apoE and cav-1. Inclusion of non-immune serum in the immunoprecipitation does not lead to detectable apoE or cav-1 in subsequent Western blot. Inclusion of anti-cav1 antibody leads to detection of cav-1 in Western blot, as well as a signal for apoE co-immunoprecipitated with cav-1. Inclusion of the cross-linking reagent markedly increases the amount of apoE that can be co-immunoprecipitated using an antibody to cav-1. In Fig. 2B, adipocytes were treated with the cleavable cross-linker DSP, and cell lysates were prepared using denaturing conditions in SDS prior to immunoprecipitation with an antibody to apoE. After immunoprecipitation, the cross-linker was cleaved and the immunoisolate was

utilized for cav-1 and apoE Western blot. Inclusion of non-immune serum in the immunoprecipitation does not produce detectable cav-1 or apoE in subsequent Western blots. Addition of apoE antibody to the immunoprecipitation produces detectable apoE and cav-1. The amount of cav-1 brought down by the apoE antibody is markedly increased in the presence of the cross-linking reagent. In Fig. 2C, 3T3-L1 adipocytes were incubated in basal medium or CH for 2h prior to harvest, and total cell lysates were used for Western blot. As shown here, a 2h incubation in CH produces no change in total cell caveolin or apoE. In view of the results in Fig. 1, we next examined how this 2h incubation in CH influences the co-immunoprecipitation of these two proteins. In Fig. 2D, cells were incubated in basal medium or basal medium plus CH for 2h. Cell lysates were prepared using non-denaturing conditions incubated with an antibody to apoE and the immune complexes were isolated on protein G beads. The resultant immunoisolate was then denatured and utilized for Western blotting for cav-1. After cell incubation in BSA, cav-1 is detected after immunoprecipitation of apoE under non-denaturing conditions. However, consistent with the confocal images, incubation of intact cells with CH prior to lysis of cells increases the amount cav-1 immunoprecipitated with apoE by approximately 4-fold.

Figure 3 shows the results of experiments using discontinuous sucrose gradients to isolate caveolae in order to study apoE and cav-1 distribution. Discontinuous sucrose gradients were prepared as described in Methods, and twelve 1ml fractions were collected (from lower to higher density). Fractions were then utilized for Western blot of cav-1 and apoE. Cav-1 was detected only in light density membrane fractions 3 and 4, with very little in higher density fractions. ApoE could also be detected in low-density membrane fractions, but could also be detected in higher density fractions 9-12. Fig. 3B shows the change in subcellular distribution of apoE

produced by incubating intact cells with CH prior to subcellular fractionation. Compared to incubation in BSA alone, the addition of CH leads to a marked re-distribution of apoE from high-density to the low-density membrane fractions 3, 4, and 5. In four similar experiments, the fraction of total adipocyte apoE found in the caveolar fraction was 15-25% under basal conditions, but increased to >60% after incubation of intact cells with CH for 2h. Incubation in a long-chain polyunsaturated fatty acid (18:2, linoleic acid) or a short-chain saturated fatty acid (16:0, palmitic acid) at concentrations sufficient to perturb adipocyte TG turnover (not shown) did not lead to apoE redistribution to the caveolar fraction. Fig. 3C shows the effect of incubating intact cells with cyclodextrin prior to subcellular fractionation. Removal of cellular CH with cyclodextrin leads to reduction of cav-1 in the low-density membrane fractions and its redistribution throughout the gradient. Incubation in cyclodextrin also leads to loss of apoE in low-density membrane fractions.

In view of the dramatic redistribution of both apoE and cav-1 in response to cyclodextrin, we wished to determine if this short-term (50 min) incubation influenced either total cellular level of either protein, and if the apoE and cav-1 translocated out of the plasma membrane after cyclodextrin treatment remain co-localized. Fig. 3D shows that total cellular levels of apoE and cav-1 were not influenced by incubation of cells to cyclodextrin for 50 minutes. Therefore, loss of both of these proteins in the caveolar fraction can be completely accounted for by the redistribution to higher density fractions. We next performed a non-denaturing co-immunoprecipitation to evaluate the degree of co-localization of apoE and cav-1 in cells treated with cyclodextrin. As shown in Fig. 3E, the incubation in cyclodextrin leads to substantial reduction in their co-localization as detected by non-denaturing co-immunoprecipitation; consistent with results using confocal microscopy.

We next directly reduced adipocyte cav-1 expression using a silencing RNA approach. Fig. 4A shows the time course for reduction of cav-1 protein in cells treated with a silencing compared to a control siRNA. Cav-1 protein levels are reduced by greater than 90% at 36h, and the reduction is maintained for at least 72h. The control silencing RNA produced no change in cav-1 mRNA. Fig. 4B shows that treatment of cells with the cav-1 silencing RNA (shown in the bottom panels) leads to almost complete loss of apoE from the plasma membrane and its redistribution to the intracellular space. Moreover, after silencing of cav-1, incubation of adipocytes with CH fails to mobilize apoE to the adipocyte plasma membrane (right panel, Fig. 4).

Amino acids 80 to 101 of cav-1, termed its scaffolding domain, have been shown to non-covalently interact with a number of proteins that can be reversibly localized to caveolae (7,28-30). Many of these interacting proteins contain a domain enriched in aromatic amino acids and several spacing motifs for these have been described. The human apoE sequence between amino acid residues 44 and 63 is highly enriched in aromatic amino acids and this N-terminal enrichment is conserved across multiple species (Fig 5A). In view of our co-localization results for cav-1 and apoE, we evaluated the ability of amino acid residues 44-63 in human apoE to bind adipocyte cav-1. Adipocyte cell extracts were prepared in non-denaturing buffer and a biotin-labeled apoE 20-mer containing amino acids 44-63 (designated as B-CBDE in Fig 5) was added for 90 min. After incubation with NeutrAvidin beads, the amount of cav-1 in the biotin-associated complex was analyzed by Western blot. As shown in figure 5B, in the absence of added B-CBDE no cav-1 is detected in the biotin-associated complex. However, addition of increasing amounts of B-CBDE to the adipocyte lysate produced increasing amounts of cav-1 in the biotin-associated complex, with saturation detected at 1 $\mu$ M. The addition of a two-fold

excess of unbiotinylated 20-mer (CBDE in Fig 5) successfully competed out immobilization of cav-1 in the biotin-associated complex (Fig. 5C). In order to more definitively address the need for the aromatic amino acids in CBDE, an apoE 20-mer of amino acids 44 to 63 was prepared in which all of the aromatic residues were changed to glycine (CBDE-mut in Fig 5). The mutant or native 20-mers were then used in a competition assay (shown in Fig 5D). The native 20-mer effectively competed for immobilization of cav-1 in the biotin-associated complex while the mutant was completely ineffective. These results indicate that the apoE domain between amino acid residues 44 and 63 saturably and specifically binds cav-1 in adipocyte lysates in a manner critically dependent on the presence of aromatic amino acids.

We next wished to determine if absence of apoE expression would have any impact on lipid composition of caveolae. In order to evaluate this question, caveolar fractions from adipocytes harvested from WT and EKO mouse adipose tissue were isolated on discontinuous sucrose gradients and equal amounts of caveolar protein were extracted for lipid analysis on HPLTC. The experiment was repeated a total of 3 times, and the results of this pooled analysis are shown in Fig. 6. The results of the pooled analysis demonstrate a substantial decrease of CH, TG, fatty acid, sphingomyelin, PC, PS, PI and PE from 100 $\mu$ g of protein from the caveolar fraction of EKO adipocytes.

## Discussion

The current report establishes, using different experimental models and using multiple approaches, that apoE and cav-1 are co-localized at adipocyte plasma membrane, most likely in caveolae. We also show that experimental interventions that alter cellular caveolin distribution or expression also modulate the distribution of apoE between plasma membrane and cytoplasmic cellular compartments. The association of apoE and cav-1 in caveolae is enhanced by enriching cells with CH and diminished by removing plasma membrane CH. Further, after disruption of caveolar structure using CH depletion with subsequent movement of apoE and cav-1 out of the plasma membrane, co-immunoprecipitation of these two proteins is reduced. This result suggests that their association depends on an intact plasma membrane caveolar structure. Direct silencing caveolin expression also leads to loss of apoE at the cell surface and its redistribution to the intracellular space.

Cav-1 expression is required to maintain caveolar ultra-structural characteristics and lipid composition (5,6,8,31,32). Our data indicate that endogenous adipocyte apoE expression is also required to preserve caveolar lipid composition. We have previously reported an approximate 20% reduction in caveolar membrane in EKO adipocytes by quantitatively assessing the binding of fluorescently labeled cholera toxin B to the pentasaccharide chain of N-acetylneuraminyl tetrasylceramide (GM1), a caveolar-specific lipid (23). The current results indicate that the absence of apoE expression in adipocytes leads to substantial derangement in caveolar lipid composition when compared on the basis of equal caveolar protein. Of particular interest, a subset of adipocyte caveolae has been shown to synthesize TG (13). The dramatic loss of TG in the caveolae that remain in EKO adipocytes suggests that this TG-rich caveolar subset may be most affected by the absence of apoE expression.

It is possible to get insight into the implications of the interaction between adipocyte cav-1 and apoE by considering the expression of these two proteins in other cell types. Endothelial cells express high levels of cav-1 and have abundant caveolae, but express little apoE (33). This would suggest that apoE is not necessary for maintaining structure and/or lipid composition of caveolae in all cell types; and its importance for maintaining caveolar lipid composition in adipocytes may be related to the high lipid flux and/or lipid storage for which these cells are specialized. On the other hand, macrophages express abundant apoE, but have few caveolae (34). Macrophages have large stores of CH stored mostly as CH ester, and apoE expression in macrophages is importantly involved in facilitating CH efflux (35). This would suggest that caveolae are not necessary for facilitating apoE-mediated sterol efflux from cells. Different from macrophages, adipocytes have the ability and need to store large amounts of free CH, not only to support plasma membrane structure and function, but also as a polar lipid component of the TG droplet (36-40). In fact, it has been shown that an adequate supply of free CH is required for maintaining normal TG droplet physiology in adipocytes (36-40).. A novel sterol recapture mechanism that enhances adipocyte sterol content has been shown to critically involve apoE and LRP; an apoE binding protein that can also be localized to cellular caveolae (41). In adipocytes, therefore, one can also speculate the localization of apoE in caveolae may be related to recapture and preservation of cellular CH; as CH synthesis in these cells is very low.

There are a number of mechanisms that can contribute to the localization of apoE to adipocyte caveolae. Proteins containing domains enriched in aromatic amino acids have been shown to non-covalently associate with the cav-1 scaffolding domain (7,28-30). The N-terminal portion of apoE between amino acids 44 and 63 is enriched in such amino acids similar to other proteins shown to associate with cav-1 in this manner. Fig. 5 demonstrates saturable and specific

binding of this portion of apoE to cav-1 in adipocyte lysates. Such a direct association between apoE and cav-1 is also consistent with the cross-linking between apoE and cav-1 that we demonstrate using a cross-linking radius of 1.2nM (Fig. 2B).

Other mechanisms mediating apoE localization to caveolae may also be operative and remain to be explored. CH enrichment could alter the number of caveolae or lipid composition in caveolae in a manner that increases the affinity of apoE for lipid components in the caveolar membrane. Cav-1 is a sterol binding protein and apoE binds phospholipid with high affinity, and both sterol and phospholipid are enriched in caveolae where they associate in membrane complexes. The literature provides several observations that would support such a lipid-mediated co-localization for apoE and cav-1 (8,42-44). The C-terminal domain of apoE is highly  $\alpha$ -helical and is thought to be primarily involved in mediating the association of apoE with phospholipid (42). Cav-1 has high affinity for sterol and is thought to exist not only in a membrane-associated form but also in a cytoplasmic and secreted form (8,43,44). In each of the latter two forms, cav-1 appears to exist as part of a high-density lipoprotein particle that can contain apoA1, which like apoE, is also a soluble amphipathic  $\alpha$ -helical apolipoprotein. Alternatively, a number of receptors that can directly bind to apoE may be localized to caveolae, and their distribution to caveolae may be influenced by cellular CH flux (45,46). Any mechanism considered must take into account the observation that the CH-mediated redistribution of apoE from the adipocyte cytoplasmic space to the adipocyte plasma membrane is absolutely dependent on the expression of cav-1 in these cells (Fig. 4). This observation would support the importance of a non-covalent interaction between cav-1 protein and apoE, but could also be consistent with a required role for caveolin in organizing plasma membrane lipid domains to increase their affinity for apoE.

Cav-1 expression and caveolae are necessary for preserving signaling pathways, endocytic pathways, and TG droplet metabolism in adipocytes (5-12). Endogenous expression of apoE also plays a role in preserving adipocyte caveolar lipid composition, endocytic pathways and TG droplet metabolism (21-23). The results in this manuscript provide evidence and mechanism for an unexpected interaction between two proteins involved in cellular lipid metabolism in a cell type specialized for lipid storage and flux, and rationalize a biologic and morphologic basis for observations establishing a role for endogenous adipocyte apoE in modulating adipocyte lipid metabolism (16,21-23).

## **Acknowledgments**

The authors thank Stephanie Thompson for assistance with manuscript preparation. This work was supported by grant DK71711 (to TM) from the National Institutes of Health.

## REFERENCES

1. Fantuzzi, G. and T. Mazzone. 2007. Adipose tissue and atherosclerosis - exploring the connection. *Arterioscler. Thromb. Vasc. Biol.* **27**: 996-1003.
2. Ogden, C. L., M. D. Carroll, and K. M. Flegal. 2003. Epidemiologic trends in overweight and obesity. *Endocrinol. Metab. Clin. North Am.* **32**: 741-760.
3. Scherer, P. E. 2006. Adipose Tissue: from lipid storage compartment to endocrine organ. *Diabetes.* **55**: 1537-1545.
4. Berg, A. H. and P. E. Scherer. 2005. Adipose tissue, inflammation, and cardiovascular disease. *Circ. Res.* **96**: 939-949.
5. Williams, T. M. and M. P. Lisanti. 2004. The caveolin proteins. *Genome Biol.* **5**: 214.
6. Pilch, P. F., R. P. Souto, L. Liu, M. P. Jedrychowski, E. A. Berg, C. E. Costello, and S. P. Gygi. 2007. Cellular spelunking: exploring adipocyte caveolae. *J. Lipid Res.* **48**: 2103-2111.
7. Liu, P., M. Rudick, and R. G. Anderson. 2002. Multiple functions of caveolin-1. *J. Biol. Chem.* **277**: 41295-41298.
8. Shigematsu, S., R. T. Watson, A. H. Khan, and J. E. Pessin. 2003. The adipocyte plasma membrane caveolin functional/structural organization is necessary for the efficient endocytosis of GLUT4. *J. Biol Chem.* **278**: 10683-10690.
9. Gonzalez-Munoz, E., C. Lopez-Iglesias, M. Calvo, M. Palacin, A. Zorzano, and M. Camps. 2009. Caveolin-1 loss of function accelerates glucose transporter 4 and insulin receptor degradation in 3T3-L1 adipocytes. *Endocrinology.* **150**: 3493-3502.
10. Razani, B., T. P. Combs, X. B. Wang, P. G. Frank, D. S. Park, R. G. Russell, M. Li, B. Tang, L. A. Jelicks, P. E. Scherer, and M. P. Lisanti. 2002. Caveolin-1-deficient mice are

- lean, resistant to diet-induced obesity, and show hypertriglyceridemia with adipocyte abnormalities. *J. Biol. Chem.* **277**: 8635-8647.
11. Le, L. S., C. M. Blouin, E. Hajduch, and I. Dugail. 2009. Filling up adipocytes with lipids. Lessons from caveolin-1 deficiency. *Biochim. Biophys. Acta.* **1791**: 514-518.
  12. Cohen, A. W., B. Razani, X. B. Wang, T. P. Combs, T. M. Williams, P. E. Scherer, and M. P. Lisanti. 2003. Caveolin-1-deficient mice show insulin resistance and defective insulin receptor protein expression in adipose tissue. *Am. J. Physiol. Cell Physiol.* **285**: C222-C235.
  13. Ost, A., U. Ortegren, J. Gustavsson, F. H. Nystrom, and P. Stralfors. 2005. Triacylglycerol is synthesized in a specific subclass of caveolae in primary adipocytes. *J. Biol. Chem.* **280**: 5-8.
  14. Zechner, R., R. Moser, T. C. Newman, S. K. Fried, and J. L. Breslow. 1991. Apolipoprotein E gene expression in mouse 3T3-L1 adipocytes and human adipose tissue and its regulation by differentiation and lipid content. *J. Biol. Chem.* **266**: 10583-10588.
  15. Yue, L., N. Rassouli, G. Ranganathan, P. A. Kern, and T. Mazzone. 2004. Divergent effects of PPAR agonists and TNF on adipocyte apoE expression. *J. Biol. Chem.* **279**: 47626-47632.
  16. Huang, Z. H., R. M. Luque, R. D. Kineman, and T. Mazzone. 2007. Nutritional regulation of adipose tissue apolipoprotein E expression. *Am. J. Physiol. Endocrinol. Metab.* **293**: E203-E209.
  17. Rao, P., Z. H. Huang, and T. Mazzone. 2007. Angiotensin II regulates adipocyte apolipoprotein E expression. *J. Clin. Endocrinol. Metab.* **92**: 4366-4372.

18. Yue, L., J. W. Christman, and T. Mazzone. 2008. Tumor necrosis factor- $\alpha$ -mediated suppression of adipocyte apolipoprotein E gene transcription: primary role for the nuclear factor (NF)- $\kappa$ B pathway and NF $\kappa$ B p50. *Endocrinology*. **149**: 4051-4058.
19. Espiritu, D. J. and T. Mazzone. 2008. Oxidative stress regulates adipocyte apolipoprotein E and suppresses its expression in obesity. *Diabetes*. **57**: 2992-2998.
20. Yue, L. and T. Mazzone. 2009. Peroxisome proliferator-activated receptor  $\gamma$  stimulation of adipocyte ApoE gene transcription mediated by the liver receptor X pathway. *J. Biol. Chem*. **284**: 10453-10461.
21. Huang, Z. H., C. A. Reardon, and T. Mazzone. 2006. Endogenous apoE expression modulates adipocyte triglyceride content and turnover. *Diabetes*. **55**: 3394-3402.
22. Huang, Z. H., D. Gu, and T. Mazzone. 2009. Role of adipocyte-derived apoE for modulating adipocyte size, lipid metabolism, and gene expression *in vivo*. *Am. J. Physiol. Endocrinol. Metab*. **296**: E1110-E1119.
23. Huang, Z. H., R. D. Minshall, and T. Mazzone. 2009. Mechanism for endogenously expressed APOE modulation of adipocyte VLDL metabolism: role in endocytic and lipase-mediated metabolic pathways. *J. Biol. Chem*. **284**: 31512-31522.
24. Oka, Y. and M. P. Czech. 1984. Photoaffinity labeling of insulin-sensitive hexose transporters in intact rat adipocytes. Direct evidence that latent transporters become exposed to the extracellular space in response to insulin. *J. Biol. Chem*. **259**: 8125-8133.
25. Song, K. S., S. Li, T. Okamoto, L. A. Quilliam, M. Sargiacomo, and M. P. Lisanti. 1996. Co-purification and direct interaction of Ras with caveolin, an integral membrane protein of caveolae microdomains. Detergent-free purification of caveolae microdomains. *J. Bioll Chem*. **271**: 9690-9697.

26. Mazzone, T., L. Pustelnikas, and C. A. Reardon. 1992. Post-translational regulation of macrophage apoprotein E production. *J. Biol. Chem.* **267**: 1081-1087.
27. Hovanessian, A. G., J. P. Briand, E. A. Said, J. Svab, S. Ferris, H. Dali, S. Muller, C. Desgranges, and B. Krust. 2004. The caveolin-1 binding domain of HIV-1 glycoprotein gp41 is an efficient B cell epitope vaccine candidate against virus infection. *Immunity.* **21**: 617-627.
28. Bucci, M., J. P. Gratton, R. D. Rudic, L. Acevedo, F. Roviezzo, G. Cirino, and W. C. Sessa. 2000. In vivo delivery of the caveolin-1 scaffolding domain inhibits nitric oxide synthesis and reduces inflammation. *Nat. Med.* **6**: 1362-1367.
29. Couet, J., S. Li, T. Okamoto, T. Ikezu, and M. P. Lisanti. 1997. Identification of peptide and protein ligands for the caveolin-scaffolding domain. Implications for the interaction of caveolin with caveolae-associated proteins. *J. Biol. Chem.* **272**: 6525-6533.
30. Bernatchez, P. N., P. M. Bauer, J. Yu, J. S. Prendergast, P. He, and W. C. Sessa. 2005. Dissecting the molecular control of endothelial NO synthase by caveolin-1 using cell-permeable peptides. *Proc. Natl. Acad. Sci. U. S. A.* **102**: 761-766.
31. Razani, B., J. A. Engelman, X. B. Wang, W. Schubert, X. L. Zhang, C. B. Marks, F. Macaluso, R. G. Russell, M. Li, R. G. Pestell, V. D. Di, H. Hou, Jr., B. Kneitz, G. Lagaud, G. J. Christ, W. Edelmann, and M. P. Lisanti. 2001. Caveolin-1 null mice are viable but show evidence of hyperproliferative and vascular abnormalities. *J. Biol. Chem.* **276**: 38121-38138.
32. Drab, M., P. Verkade, M. Elger, M. Kasper, M. Lohn, B. Lauterbach, J. Menne, C. Lindschau, F. Mende, F. C. Luft, A. Schedl, H. Haller, and T. V. Kurzchalia. 2001. Loss

- of caveolae, vascular dysfunction, and pulmonary defects in caveolin-1 gene-disrupted mice. *Science*. **293**: 2449-2452.
33. Minshall, R. D., W. C. Sessa, R. V. Stan, R. G. Anderson, and A. B. Malik. 2003. Caveolin regulation of endothelial function. *Am. J. Physiol. Lung Cell. Mol. Physiol.* **285**: L1179-L1183.
34. Kockx, M., W. Jessup, and L. Kritharides. 2008. Regulation of endogenous apolipoprotein E secretion by macrophages. *Arterioscler. Thromb. Vasc. Biol.* **28**: 1060-1067.
35. Lin, C.-Y., H. Duan, and T. Mazzone. 1999. Apolipoprotein E-dependent cholesterol efflux from macrophages: Kinetic analysis and divergent mechanism for endogenous versus exogenous apolipoprotein E. *J. Lipid Res.* **40**: 1618-1626.
36. Prattes, S., G. Horl, A. Hammer, A. Blaschitz, W. F. Graier, W. Sattler, R. Zechner, and E. Steyrer. 2000. Intracellular distribution and mobilization of unesterified cholesterol in adipocytes: triglyceride droplets are surrounded by cholesterol-rich ER-like surface layer structures. *J. Cell. Sci.* **113**: 2977-2989.
37. Le Lay, S., S. Krief, C. Farnier, I. Lefrere, X. Liepvre, R. Bazin, P. Ferre, and E. Dugail. 2001. Cholesterol: a cell size dependent signal which regulates glucose metabolism and gene expression in adipocytes. *J. Biol. Chem.* **276**: 16904-16910.
38. Le, L. S., P. Ferre, and I. Dugail. 2004. Adipocyte cholesterol balance in obesity. *Biochem. Soc. Trans.* **32**: 103-106.
39. Juvet, L. K., S. M. Andresen, G. U. Schuster, K. T. Dalen, K. A. Tobin, K. Hollung, F. Haugen, S. Jacinto, S. M. Ulven, K. Bamberg, J. A. Gustafsson, and H. I. Nebb. 2003. On

- the role of liver X receptors in lipid accumulation in adipocytes. *Mol. Endocrinol.* **17**: 172-182.
40. Dugail, I., L. S. Le, M. Varret, L. Le, X, G. Dagher, and P. Ferre. 2003. New insights into how adipocytes sense their triglyceride stores. Is cholesterol a signal? *Horm. Metab. Res.* **35**: 204-210.
41. Vassiliou, G. and R. McPherson. 2004. A novel efflux-recapture process underlies the mechanism of high-density lipoprotein cholesteryl ester-selective uptake mediated by the low-density lipoprotein receptor-related protein. *Arterioscler. Thromb. Vasc. Biol.* **24**: 1669-1675.
42. Hatters, D. M., C. A. Peters-Libeu, and K. H. Weisgraber. 2006. Apolipoprotein E structure: insights into function. *Trends Biochem. Sci.* **31**: 445-454.
43. Ito, J., Y. Nagayasu, K. Kato, R. Sato, and S. Yokoyama. 2002. Apolipoprotein A-I induces translocation of cholesterol, phospholipid, and caveolin-1 to cytosol in rat astrocytes. *J. Biol. Chem.* **277**: 7929-7935.
44. Frank, P. G., M. W. Cheung, S. Pavlides, G. Llaverias, D. S. Park, and M. P. Lisanti. 2006. Caveolin-1 and regulation of cellular cholesterol homeostasis. *Am. J. Physiol. Heart Circ. Physiol.* **291**: H677-H686.
45. Zhang, H., P. H. Links, J. K. Ngsee, K. Tran, Z. Cui, K. W. Ko, and Z. Yao. 2004. Localization of low density lipoprotein receptor-related protein 1 to caveolae in 3T3-L1 adipocytes in response to insulin treatment. *J. Biol. Chem.* **279**: 2221-2230.
46. Boucher, P., P. Liu, M. Gotthardt, T. Hiesberger, R. G. Anderson, and J. Herz. 2002. Platelet-derived growth factor mediates tyrosine phosphorylation of the cytoplasmic

domain of the low density lipoprotein receptor-related protein in caveolae. *J. Biol. Chem.*  
**277**: 15507-15513.

## Figure Legends

**Figure 1. Cellular localization of adipocyte apoE and cav-1 under basal and CH-enriched conditions.** Adipocytes were incubated in 100 $\mu$ M BSA/DMEM or this medium containing 10 $\mu$ g/ml CH for 2h or 10mM M $\beta$ CD for 50 min as indicated. A. Cultures of primary rat adipocytes were stained with anti-apoE or anti-cav-1 and used for confocal microscopy as described in Methods. B. 3T3-L1 adipocytes were stained with anti-apoE or anti-cav-1 and used for confocal microscopy as described in Methods. C. Endogenously synthesized apoE was detected in 3T3-L1 cells after expression of an apoE-GFP protein. Cells were also stained with anti-cav-1 as described in Methods. D. Plasma membrane sheets were isolated (as described in Methods) after incubation of intact 3T3-L1 cells under basal conditions or with CH, or with M $\beta$ CD. Plasma membrane sheets were stained with anti-apoE and anti-cav-1 and imaged with confocal microscopy.

**Figure 2. Co-immunoprecipitation of apoE and cav-1.** A. 3T3-L1 cells were incubated in 100 $\mu$ M BSA for 2h. After this incubation, cells were lysed in non-denaturing buffer and the lysate was for immunoprecipitation using non-immune serum or anit-cav1 antibody as indicated. Where indicated, 3T3-L1 cells were treated with the cell permeant reducible cross-linker DSP prior to lysis in denaturing but non-reducing buffer. The immunoprecipitates were eluted from protein G agarose beads in denaturing buffer containing 5% DMEM to cleave the cross-linker. The eluates were then separated on an SDS-PAGE and utilized for Western blot of cav-1 and apoE. B. 3T3-L1 cells were treated with the cell permeant reducible cross-linker DSP, as described in Methods. Cells were lysed using denaturing conditions (but without reducing

agents) and immunoprecipitated with an antibody to apoE. The immunoprecipitates were eluted from protein G agarose beads in denaturing buffer containing 5% BME to cleave the cross-linker. The eluates were then separated on SDS-PAGE and utilized for Western blot of cav-1 and apoE. C. 3T3-L1 cells were incubated in 100 $\mu$ M BSA alone, or this medium plus 10 $\mu$ g/ml CH for 2h. After this incubation, cell lysates were used for Western blot for apoE and cav-1 as indicated. D. 3T3-L1 cells were incubated in 100 $\mu$ M BSA alone, or this medium plus 10 $\mu$ g/ml CH for 2h. After this incubation, cells were lysed in non-denaturing buffer and immunoprecipitated with an antibody to apoE. The immunoprecipitates were eluted from protein G agarose beads using denaturing and reducing conditions. The eluates were separated on SDS gels and used for Western blot for cav-1, and apoE

**Figure 3. Cav-1 and apoE distribution in adipocyte caveolae isolated on discontinuous sucrose gradients.** 3T3-L1 adipocytes were homogenized and separated on discontinuous sucrose gradients as described in Methods. Fractions collected from the gradient (going from lower to higher density) were utilized for Western blot for apoE and/or cav-1. A. Distribution of cav-1 and apoE in fractions collected from cells incubated in BSA. The distribution of each protein across the fractions is shown as a percentage in the graph below the Western blot. B. ApoE distribution in the sucrose density fractions was measured in cells that were preincubated in BSA alone, with 10 $\mu$ g/ml CH, or with 250 $\mu$ M albumin bound linoleic or palmitic acid (FFA:BSA molar ratio 2.5:1) for 2h. The percent of apoE in fractions from cells incubated with BSA or CH is shown in the graph below the Western blot. C. ApoE and cav-1 distribution in the gradient fractions after preincubation of cells in 10mM M $\beta$ CD for 50 min. D. 3T3-L1 cells were incubated in BSA or this medium plus 10mM M $\beta$ CD for 50 min. Panel shows Western blot for

total cellular apoE and cav-1 in the two incubation conditions. E. Amount of cav-1 co-immunoprecipitated with apoE (under non-denaturing conditions as described in Methods) in cells incubated with or without M $\beta$ CD.

**Figure 4. Knockdown of cav-1 expression leads to translocation of apoE to the intracellular space.** 3T3-L1 cells were incubated with a cav-1 or control siRNA as described in Methods. A. Level of expression of cav-1 in cells exposed to the cav-1 siRNA compared to control siRNA (as determined by Western blot) is shown. B. Cells exposed to control or cav-1 siRNA were stained with anti-apoE and utilized for confocal microscopy after 48h. Where indicated, cells were incubated with 10 $\mu$ g/ml CH for 2h prior to harvest.

**Figure 5. Cav-1 binding to apoE peptides.** A. Alignment of potential cav-1 binding motifs in the N-terminal of apoE from various species. CBDE = Cav-1 Binding Domain in apoE; CBDE-mut = Cav-1 Binding Domain in apoE mutated as shown; B-CBDE = biotinylated CBDE. Aromatic amino acids and their glycine replacements are underlined in bold. B. Twenty  $\mu$ g of adipocyte extract were incubated with the indicated concentration of B-CBDE for 90 min at 4 $^{\circ}$ C. After isolation on NeutrAvidin beads, the amount of cav-1 in the immobilized biotin-associated complex was analyzed by Western blot as described in Methods. C. Two  $\mu$ M of the unbiotinylated apoE 20-mer (CBDE) was added to adipocyte cell lysates for 90 min, followed by addition of 1  $\mu$ M B-CBDE. The amount of cav-1 immobilized in the biotin complex was analyzed as described for panel B. D. Twenty  $\mu$ g of adipocyte extract were preincubated with 0.5, 1 or 2  $\mu$ M CBDE, or CBDE-mut for 90 min before addition of 1  $\mu$ M of B-CBDE for an

additional 90 min. The amount of cav-1 immobilized in the biotin-associated complex was analyzed as described above.

**Figure 6. Caveolar lipid composition in adipocytes isolated from control or EKO mature adipocytes.** Adipose tissue from two mice of each genotype was pooled in order to isolate 100µg of adipocyte caveolar protein for lipid analysis. Lipids were extracted and run on HPLTC plates as described in Methods. Densitometric analysis of pooled results of the same experiment repeated a total of 3 times, and quantitated as described in Methods.

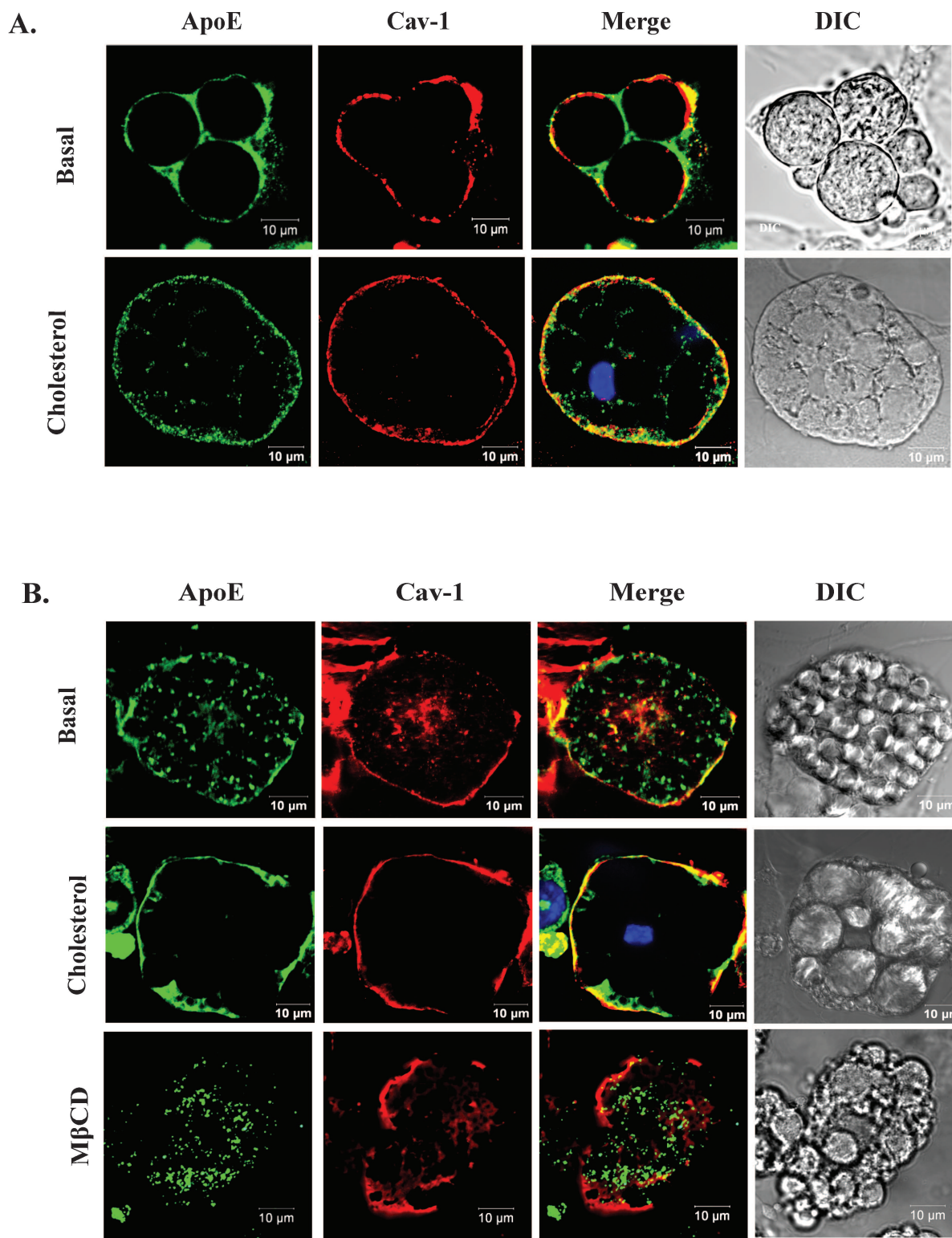
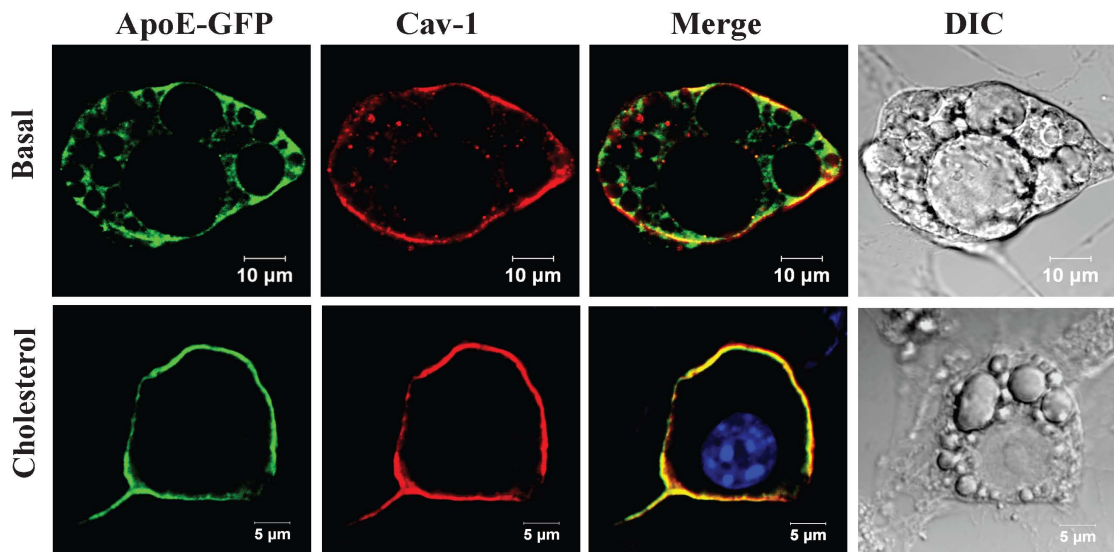


Fig. 1

**C.**



**D.**

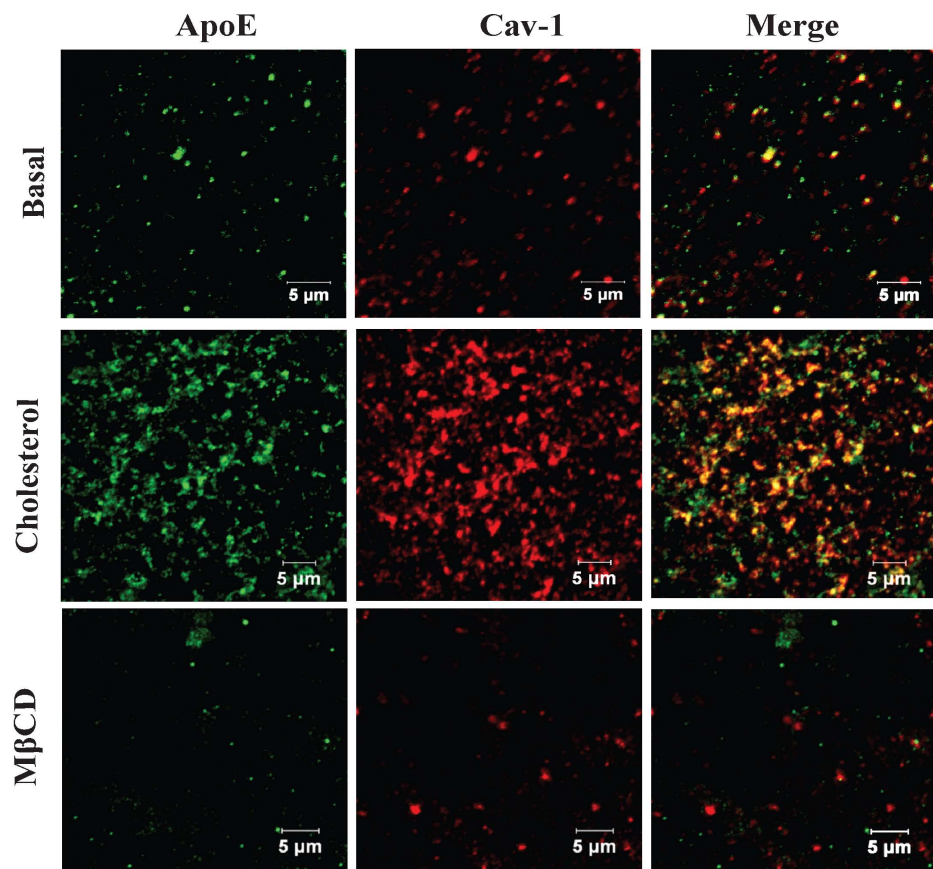
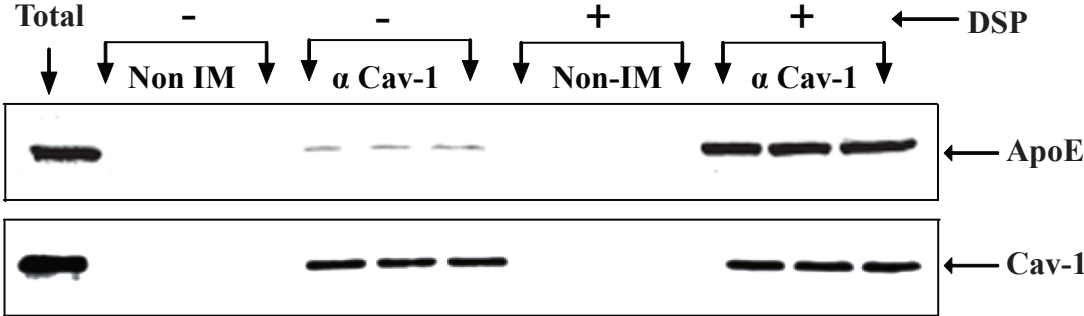


Fig.1

**A. IP: Cav-1**



**B. IP: ApoE**

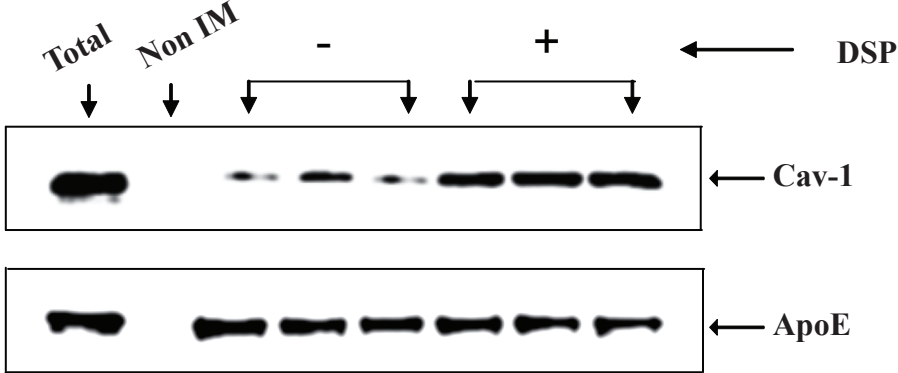
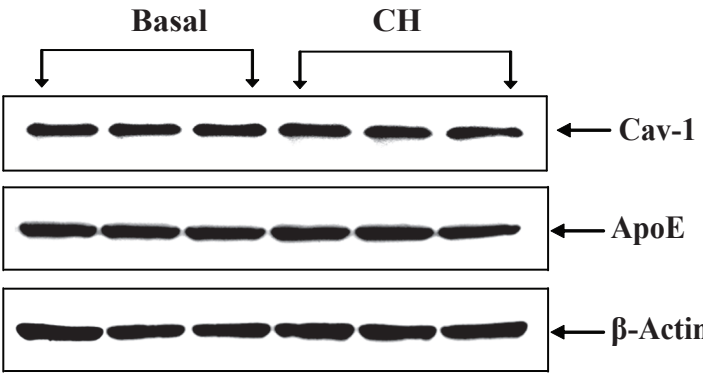


Fig. 2

**C. WB: total cell lysate**



**D. IP: ApoE**

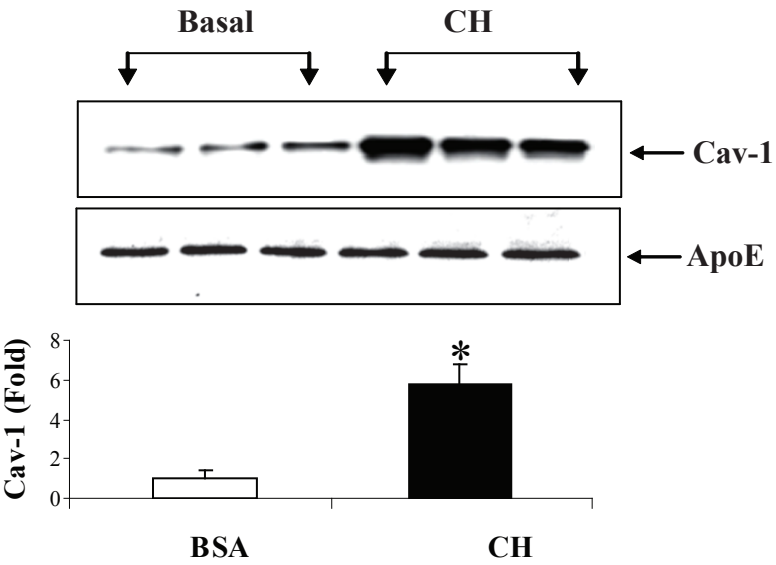


Fig. 2

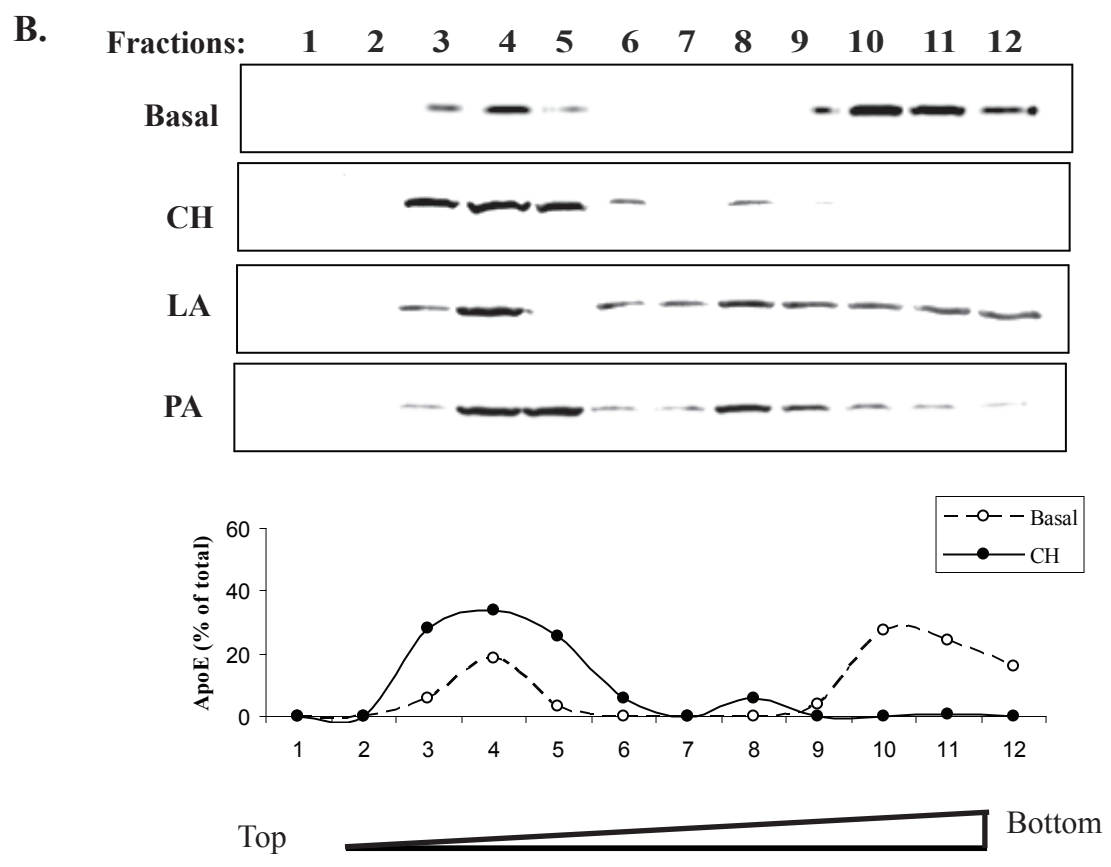
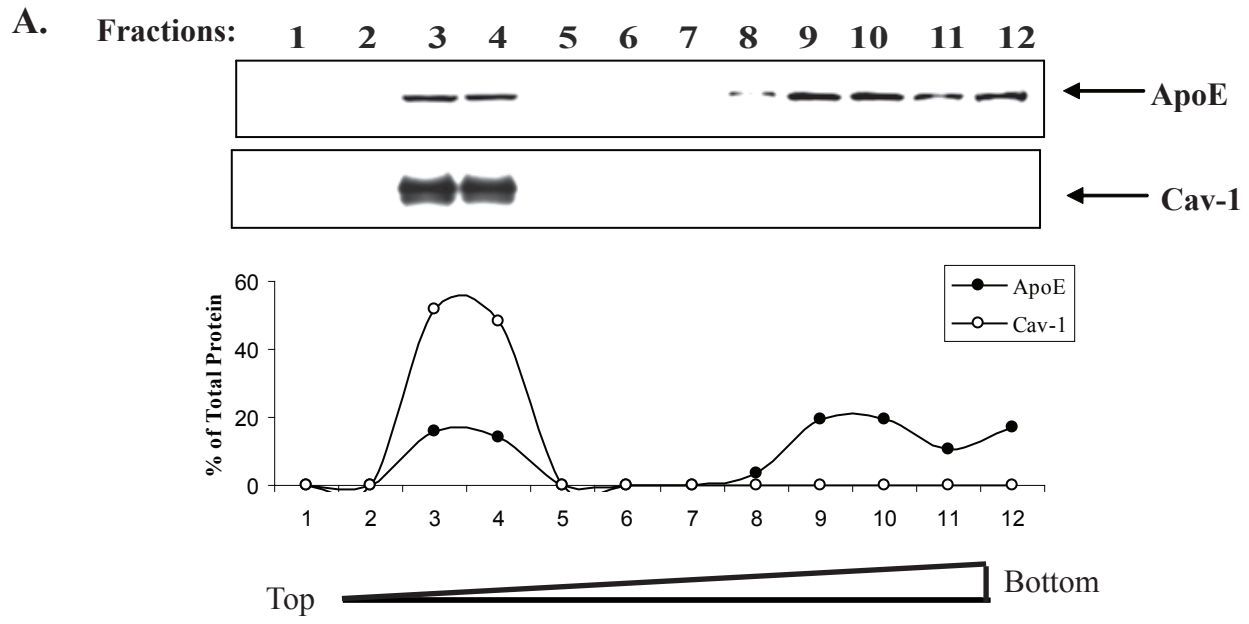
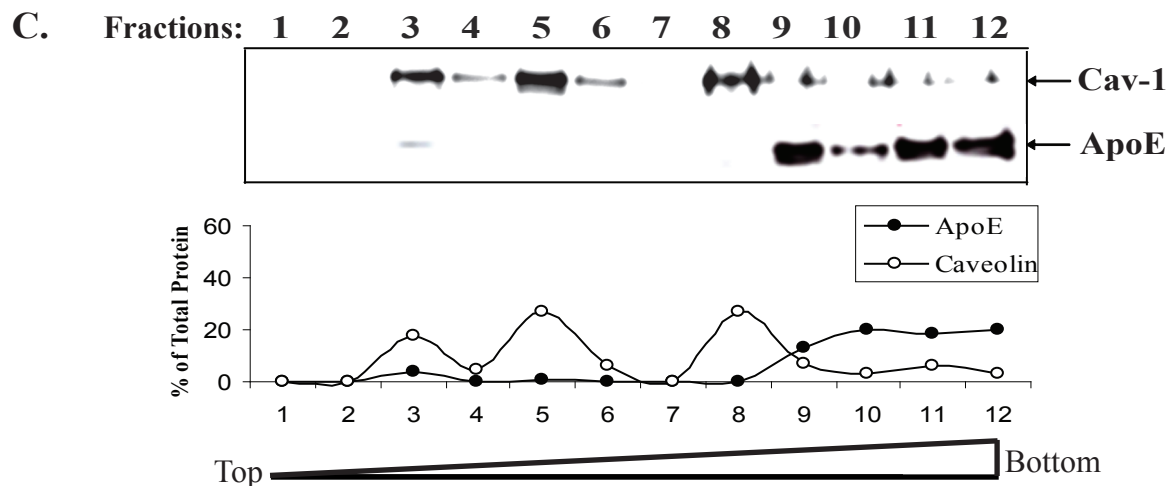
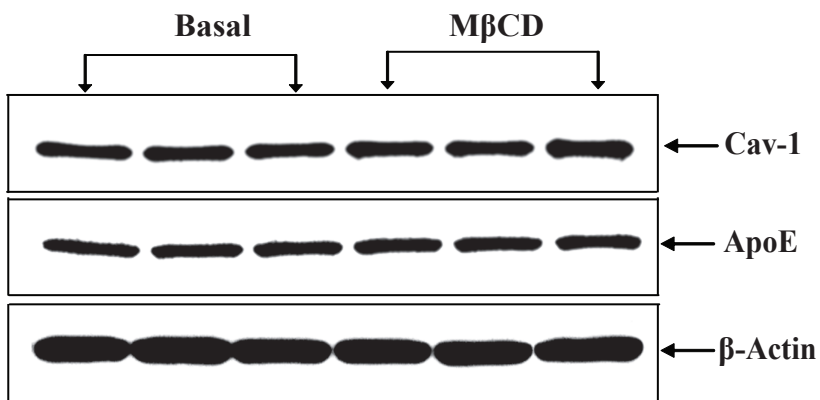


Fig. 3



**D. WB: total cell lysate**



**E. IP: ApoE**

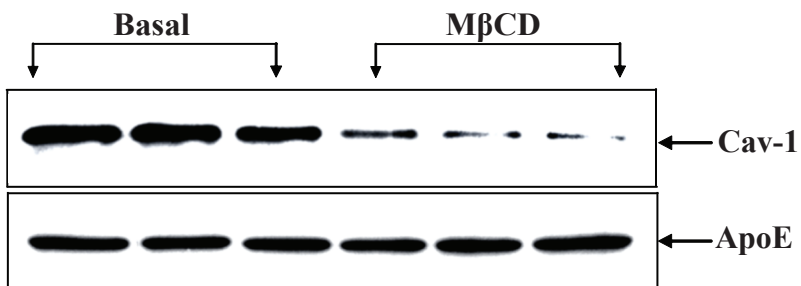
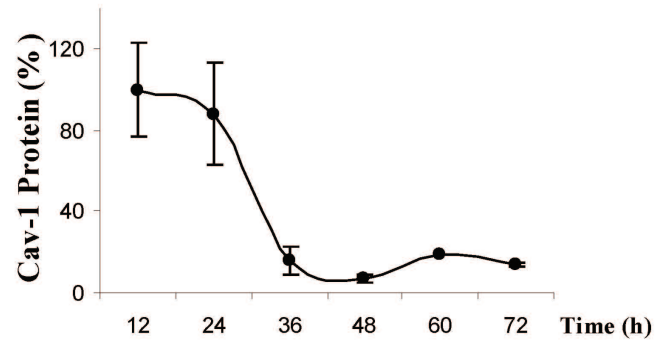


Fig. 3

**A.**



**B.**

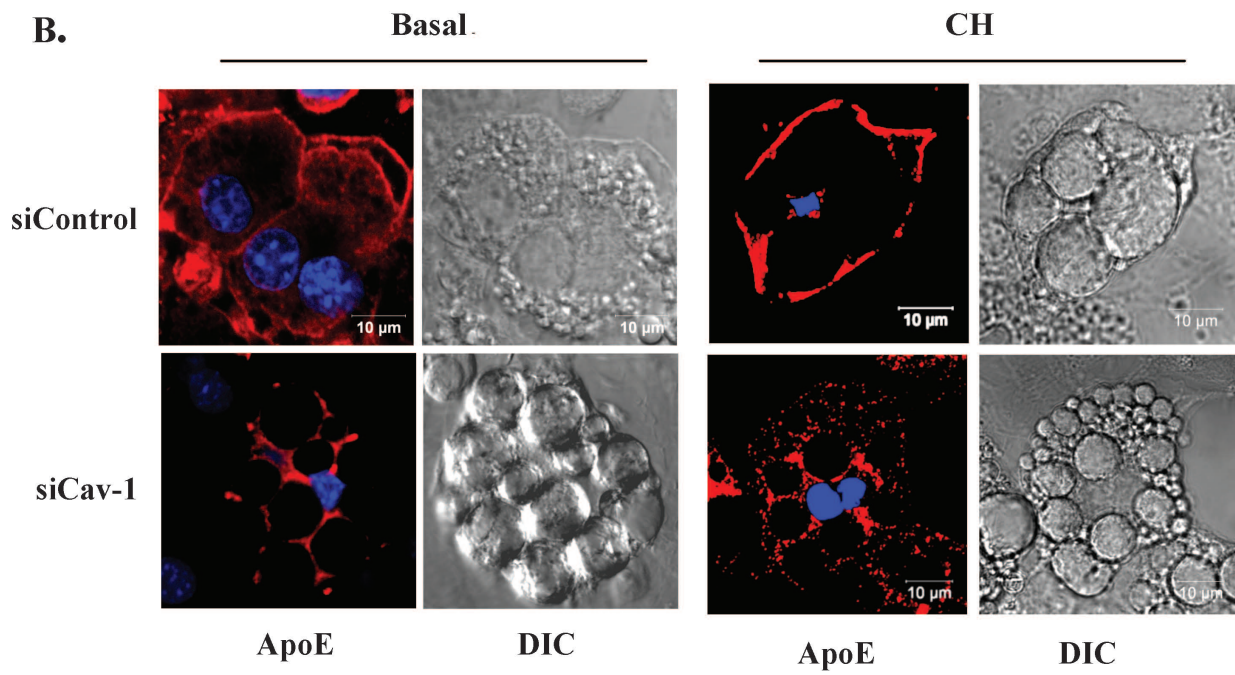


Fig. 4

**A.** Alignment of Potential Cav-1 Binding Motifs in ApoE:

Human: GQRWELALGRFWDYLRWVQT  
 Mouse: NQPWEQALNRFWDYLRWVQT  
 Rat: DQPWEQALNRFWDYLRWVQT  
 Bovine: SQPWEQALGRFWDYLRWVQT  
 Dog: GQPWEALARFWDYLRWVQT  
 Chimpanzee: GQRWELALGHFWDYLRWVQT

CBDE: GQRWELALGRFWDYLRWVQT  
 CBDE mut: GQRGELALGRGGDGLRGVQT  
 B-CBDE: Biotin-GQRWELALGRFWDYLRWVQT

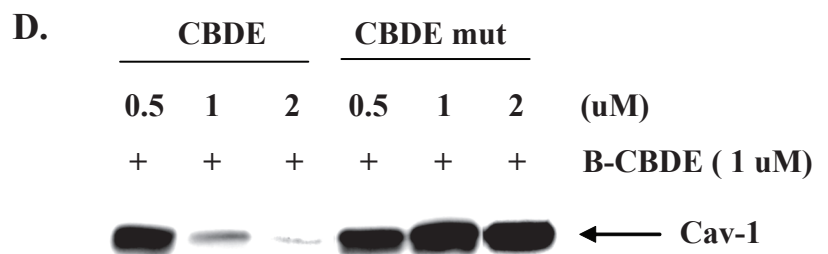
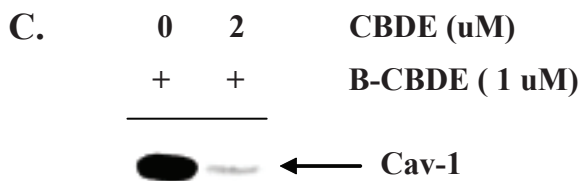
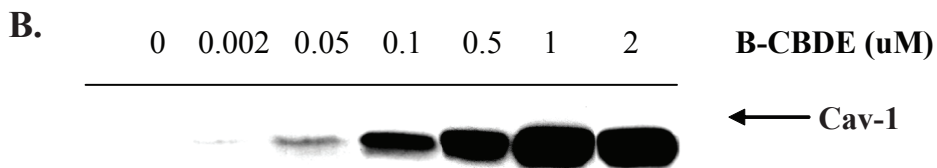


Fig. 5

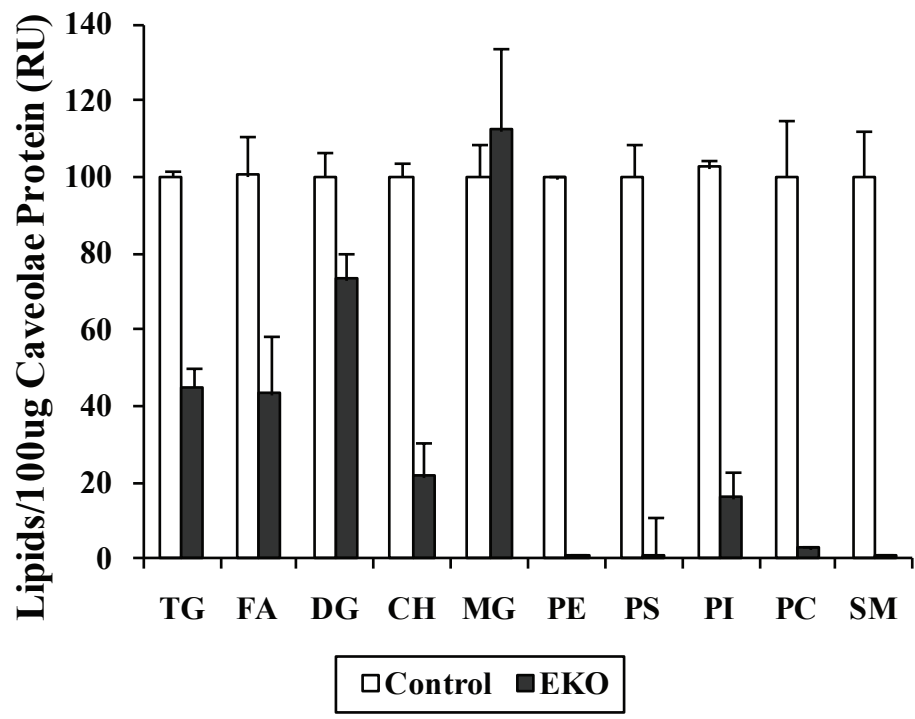


Fig. 6.